





Contents lists available at SCCE

Journal of Soft Computing in Civil Engineering

Journal homepage: www.jsoftcivil.com



Connectivity and Flowrate Estimation of Discrete Fracture Network Using Artificial Neural Network

A. Esmailzadeh^{1*} , A. Kamali², K. Shahriyar², R. Mikaeil¹ 

1. Urmia University of Technology, Urmia, Iran

2. Amirkabir University of Technology, Tehran, Iran

Corresponding author: esmailzade.ak@aut.ac.ir

 <https://doi.org/10.22115/SCCE.2018.105018.1031>

ARTICLE INFO

Article history:

Received: 08 November 2017

Revised: 03 March 2018

Accepted: 18 March 2018

Keywords:

Hydraulic parameters;

Rock mass;

Discrete fracture network (DFN);

Artificial neural network;

Connectivity.

ABSTRACT

Hydraulic parameters of rock mass are the most effective factors that affect rock mass behavioral and mechanical analysis. Aforementioned parameters include intensity and density of fracture intersections, percolation frequency, conductance parameter and mean outflow flowrate which flowing perpendicular to the hydraulic gradient direction. In order to obtain hydraulic parameters, three-dimensional discrete fracture network generator, 3DFAM, was developed. However, unfortunately, hydraulic parameters obtaining process using conventional discrete fracture network calculation is either time consuming and tedious. For this reason, in this paper using Artificial Neural Network, a tool is designed which precisely and accurately estimate hydraulic parameters of discrete fracture network. Performance of designed optimum artificial neural network is evaluated from mean Squared error, errors histogram, and the correlation between artificial neural network predicted value and with discrete fracture network conventionally calculated value. Results indicate that there is the acceptable value of mean squared error and also a major part of estimated values deviation from the actual value placed in acceptable error interval of (-1.17, 0.85). On the other hand, excellent correlation of 0.98 exists between the predicted and actual value that proves the reliability of the designed artificial neural network.

How to cite this article: Esmailzadeh A, Kamali A, Shahriar K, Mikaeil R. Connectivity and flowrate estimation of discrete fracture network using artificial neural network. J Soft Comput Civ Eng 2018;2(3):13-26. <https://doi.org/10.22115/scce.2018.105018.1031>.

2588-2872/ © 2018 The Authors. Published by Pouyan Press.

This is an open access article under the CC BY license (<http://creativecommons.org/licenses/by/4.0/>).



1. Introduction

In designing infrastructures such as dams, tunnels, and caverns which involved in the rock mass, hydraulic behavior and connectivity of fractures play important role. The significance of aforementioned parameters will be highlighted if the project site placed in zones with high pore pressure like underground caverns and tunnels of dams, underground hydrocarbon reservoirs and as well as host zones of nuclear waste. The predominantly Hydraulic behavior of discontinuous media such as rock mass is controlled by geometry and connectivity of fractures [1–5]. In rock mass hydraulic behavior study, due to inaccessibility and direct immeasurability of connectivity and flowrate, rock mass fracture network simulating using statistical fracture data such as orientation, size and spatial location and density of fracture, which named Discrete fracture network (DFN) model, is accepted and common approach [6–9]. Fracture network modeling is an important part of the design and development of natural energy resource systems including geothermal and petroleum reservoirs and aquifers [10–14]. Robinson studied fracture connectivity by percolation theory and numerical methods in 2D and tried to generalize the results to the 3D state. He considered fractures as segments which are positioned randomly in space, and their orientation follows a distinct distribution function [15]. In discrete fracture network model, percolation theory was used by several researchers such as Engelman et al., Charlaix et al., Long and Witherspoon, Stauffer. These researchers used the theory to study effects of trace length and size of fractures on the amount of fracture connectivity in 2D [3,16–18]. Bour et al. and Bour & Davy, assuming an exponential distribution function, studied different properties of fracture connectivity by percolation theory in 2D and 3D [19,20]. Darcel et al., investigated fracture connectivity in a discrete fracture network, using fractal correlation coefficients, by theoretical and numerical methods [21]. Due to the extreme importance of underground cavities for nuclear waste disposal, and to overcome uncertainties of seepage situation in the studied area, Xu et al. introduced fracture connectivity index as a parameter to quantify the state of fracture connectivity of a region [22]. Xu et al. investigated fracture connectivity in geothermal systems by discrete fracture network and studied concept and effect of this parameter on the behavior of these systems [23]. During the process of developing a discrete fracture network, they used an integrated method of Markov Chain- Monte Carlo. During their study on fracture connectivity parameter, Fadakar et al., suggested a new parameter, referred to as field fracture connectivity, which represents characteristics of true degree of spatial fracture connectivity in geothermal systems [24]. They provided some relations between field fracture connectivity, P_{21} parameter and density of discontinuities, as well. Discrete fracture network is the main element of the study in all of the above methods. However, it should be noted that, when using discrete fracture network by generating compact models to achieve a representative element volume model, the study of discrete fracture network regarding hydraulics becomes very cumbersome. Considering these conditions, obtaining a faster but considerably accurate solution is a requirement.

Addressing this need, it is attempted in this article to design an optimal neural network. Using appropriate structural properties such as proper cell model, the exact determination of suitable weighted matrix, training algorithm and an activation function, hydraulic parameters intended for discrete fracture network were generated receiving input parameters. Application of artificial

neural network (ANN) has a long history of use in different aspects of rock mechanics. Most of the investigations use the artificial neural network to predict required physical and mechanical properties. Ji et al. used ANN as an assistant tool in back-analysis method to calculate permeability tensor [25]. Benardos et al. applied ANN to predict TBM¹ performance [26]. Bowden et al. and Kingston et al. used ANN in water resources studies [27,28]. Kung et al. and Kim et al. used capabilities of ANN to estimate ground settlement due to underground excavations [29,30]. Padmini et al. used an integrated technique of Fuzzy- neural network for calculation and estimation of the ultimate bearing capacity of shallow foundations [31]. Kulatilake et al. and Menjazi et al. used ANN to predict mean size of rock fragments resulting from explosion operations in open mines [32,33]. Nejati et al. and Gokceoglu et al. used ANN to obtain deformation modulus of rock mass [34,35]. Aforementioned research works are only part of the worked paper which show the applicability of ANN in a different field of rock mechanics. This work with several other works indicates the great power of ANN in engineering disciplines. For this reasons, ANN is selected as a powerful predicting tool to overcome problems of robust calculations of DFN.

2. Artificial neural network (ANN)

Inspired by the nervous system of living organisms, Artificial Neural Networks have various capabilities. Neural networks are in fact parallel processors that perform a large amount of computation on input data. The structure of the neural network is composed of units known as neurons and neural layers that offer great flexibility and a large degree of freedom. Based on the generation of smart algorithms operation, these networks have a great capacity for correction and generalization. Many different models of neural networks were presented with various structures and algorithms. However, despite different structures, they are all similar regarding basic characteristics such as learning ability and versatility, generalizability, parallel computing, robustness, and general approximation capability [36].

Every neural network has three structural features in all of which the structure self-organization is evident: neural cell model (function type), neural network structure (topology type), and learning in the neural network (learning type). The neural cell model is determined based on the transfer function. The real output of each neuron depends on the specific transfer function that is selected, and it must satisfy the criteria required by the problem that the neural cell is used to solve [36].

All the elements of the input vector are multiplied by their weight in a neural network and are given to the transfer function or the activation function after summation by the bias of each neuron. Each layer of the neural network has an input vector, a bias vector, a weight matrix, and finally, an output vector which acts as the input vector for the next layer. In Fig 1, P represents the input vector with P_1, P_2, \dots, P_R elements. The vector \mathbf{n} is the input vector of each neuron which is obtained by multiplication of the input vector elements by the weight of each neuron. The weight matrix of the network is w_{ij}^k , where i represents the number of neurons in each layer, j

¹ Tunnel Boring Machine

represents the number of input vector elements, and k is the number of layers. Moreover, the vector **a** is the vector of outputs which is calculated by the transfer function **f** [37].

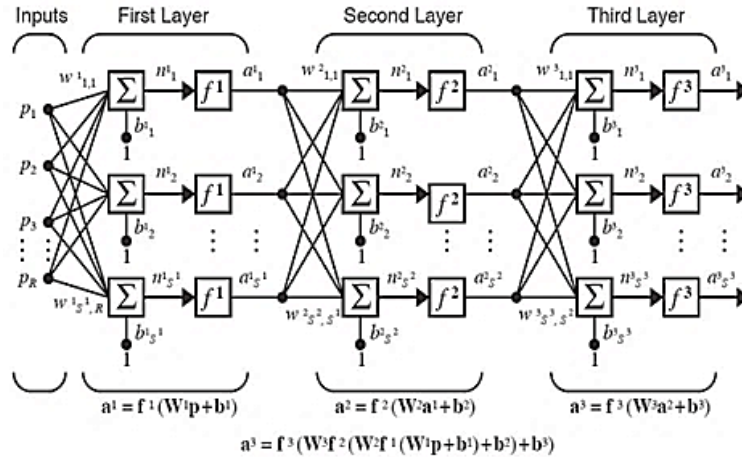


Fig. 1. Structure of multilayer Artificial Neural Network(ANN) [37].

In multilayer feedforward neural networks with backpropagation capabilities, which are commonly used in solving rock and soil mechanics problems, neurons are sorted in the form of layers including an input layer, an output layer, and one or more middle layer (hidden layers). Fig 2 shows a schematic view of a neural network.

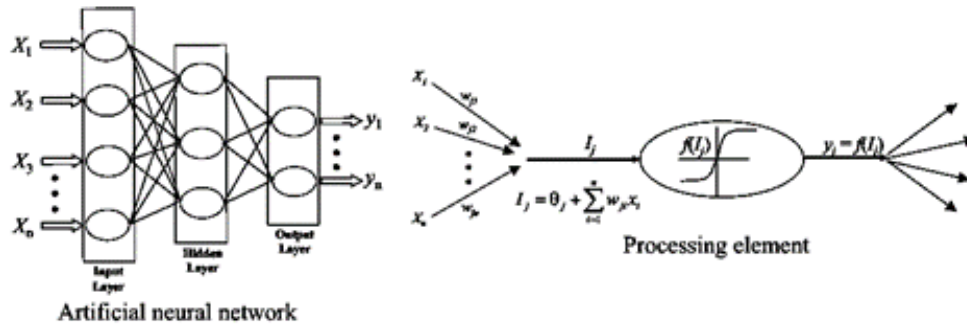


Fig. 2. ANN neurons and calculation process schematic [38].

Every processor unit (neuron) in a certain layer is connected to all or some of neurons from other layers by weights. The numerical value of the weights controls the intensity of the connection between neurons. Zero weight implies no connection among the neurons while negative weight implies no connection is allowed among them. Neurons receive weighted inputs from a large number of other neurons and send it to the transfer function after adding their bias to it; consequently, the output of the transfer function act as the input for the next layer. The bias value is applied for correct scale adjustment at neuron input, improving network convergence. Considering the artificial neural network in Fig 2, the procedure above could be presented by Eqs. 1 and 2 for neuron j [39]:

$$I_j = \theta_j + \sum_{i=1}^n w_{ji}x_i \tag{1}$$

$$y_j = f(I_j) \tag{2}$$

in which I_j is activation level of neuron j , w_{ji} is connection weights between j and i neurons, x_i is inputs from neuron i ($i = 0.1.2. \dots n$), θ_j is bias of neuron j , y_j is output of neuron j , $f(\cdot)$ is transform function [37].

3. ANN training data generation

In order to use ANN, firstly it needs to provide a series of data as network input and another series of data as network output. In this work regarding of demand data, the common and effective methodology was applied in order to create network necessary data. Data generation process and steps of data preparation are in followed parts:

3.1. Discrete fracture network (DFN) generation

In order to generate the 3D model of the fracture network, the 3D code of 3DFAM was developed in MATLAB Programming Language. In 3DFAM Code, the fractures center has been defined on the basis of modified Beacher disk and the number of fractures has been generated with the homogeneous Poisson process [7]. The uniform distribution has been used in order to simulate the fractures location in 3-D [40]. Having generated the 3D block of the discrete fracture network, it would be possible to create sections in any direction or even inclined (with any dip and dip direction) and any location. The fractures, which are situated outside the study limits, are omitted. In addition, the external trace length of the fractures, which some parts of them are inside the window, is omitted as well. The main object of truncation of the traces length is to leave out the edge effect [3].

All the trace lengths existing inside the window under consideration are studied after creating sections in the required directions. In order to study the effective connectivity between the fractures, it is needed to omit the fractures or cluster of fractures which are hydraulically inactive and do not contribute to transferring the flow after creating the section. This process is called Fractures Regulation.

Connectivity is a comprehensive parameter that is a function of orientation, size, spacing, and density of the joint sets. Such characteristics are used to define the connectivity portion in the rock mass [41]. The flow routes and the number of connected fractures along the flow routes are computed by regulating the network. In order to assess the effect of the geometrical characteristics of the fractures on the network and the parameters corresponding to the effective connectivity as well as the hydraulic conductivity of the fracture network, 3DFAM code can compute a number of these parameters for the cases before and after regulating the fractures. The percolation frequency (total connectivity) (ξ), hydraulic conductivity (η), intersection density (P_{20}), intersection intensity (P_{21}) and termination index (T_i) are the most outstanding parameters which are going to be calculated after regulating so as to study the status of the fracture network effective connectivity.

The percolation frequency is the very degree of interconnection or total connectivity of a fracture network which is computed using Relation 3:

$$\xi = \frac{n_{node}}{n} \quad (3)$$

Where n_{node} is number of intersection nodes and n is total number of fractures in fracture network [42].

The conductivity parameter, η , represents the connectivity in the fracture network. When a uniform distribution characterizes the opening, the conductivity Parameter has a linear correlation with the hydraulic conductivity of the fracture networks. This parameter is calculated using Relation 4:

$$\eta = \frac{n\bar{l}}{2} \sqrt{\frac{1+2n_{node}/n}{A}} \quad (4)$$

Where n_{node} is the number of intersection nodes, n is total number of fractures, A is the model area and \bar{l} is the arithmetic mean of all fracture lengths in fracture network [42].

The intersection density (P_{20}) and intersection intensity (P_{21}) represent the connectivity in the fracture network. These parameters are equal to the number of intersections and the sum of fracture trace length divided by the area of the fracture network.

3.2. DFN data acquisition

In order to get hold of the real conditions, four synthetic joint sets are simulated. In 84 simulations, the input data include Fisher's constant, mean and standard deviation of trace length, diameter, aperture and frequency and output parameters include percolation frequency, hydraulic conductivity, intersection density (P_{20}), intersection intensity (P_{21}) and total discharge at outflow boundary of fracture network in horizontal (Q_{13}) and vertical (Q_{24}) direction flow.

One of the most important parameters in definition of discontinuities orientation is Fisher's constant. K is the coefficient of the Fisher's constant and a positive number which indicates the degree of data scattering. The larger amount of this coefficient depicts less scattered data. The larger amount of this coefficient depicts less scattered data [43,44]. The Fisher's constant is generally in the range of 5 to 440. The range of input data variation are presented in table 1.

Table 1

Variation limits of simulations input parameters.

Fisher coefficient	Mean Trace Length(m)	Trace Length Standard Deviation(m)	Diameter(m)	Aperture(m)	Frequency (m^{-1})
5	0.77	0.21	0.99	0.0005	0.99
50	1	0.31	1.25	0.000725	1.25
100	1.27	0.4	1.6	0.000725	1.59
250	1.5	0.48	1.86	0.000725	1.86
250	1.72	0.53	1.93	0.000725	1.93

In all simulations, the shape of fractures is assumed circular, and DFN is generated in 3-D block with dimensions of $5 \times 5 \times 5 m^3$. A sample of generated DFN and a 2-D cross-section of the model in either non-regulated and regulated form is shown in figure 3. In each block, simulation

comprise 3 DFN realizations. Hence in this study that include 84 simulations, 252 realizations of DFN is analyzed.

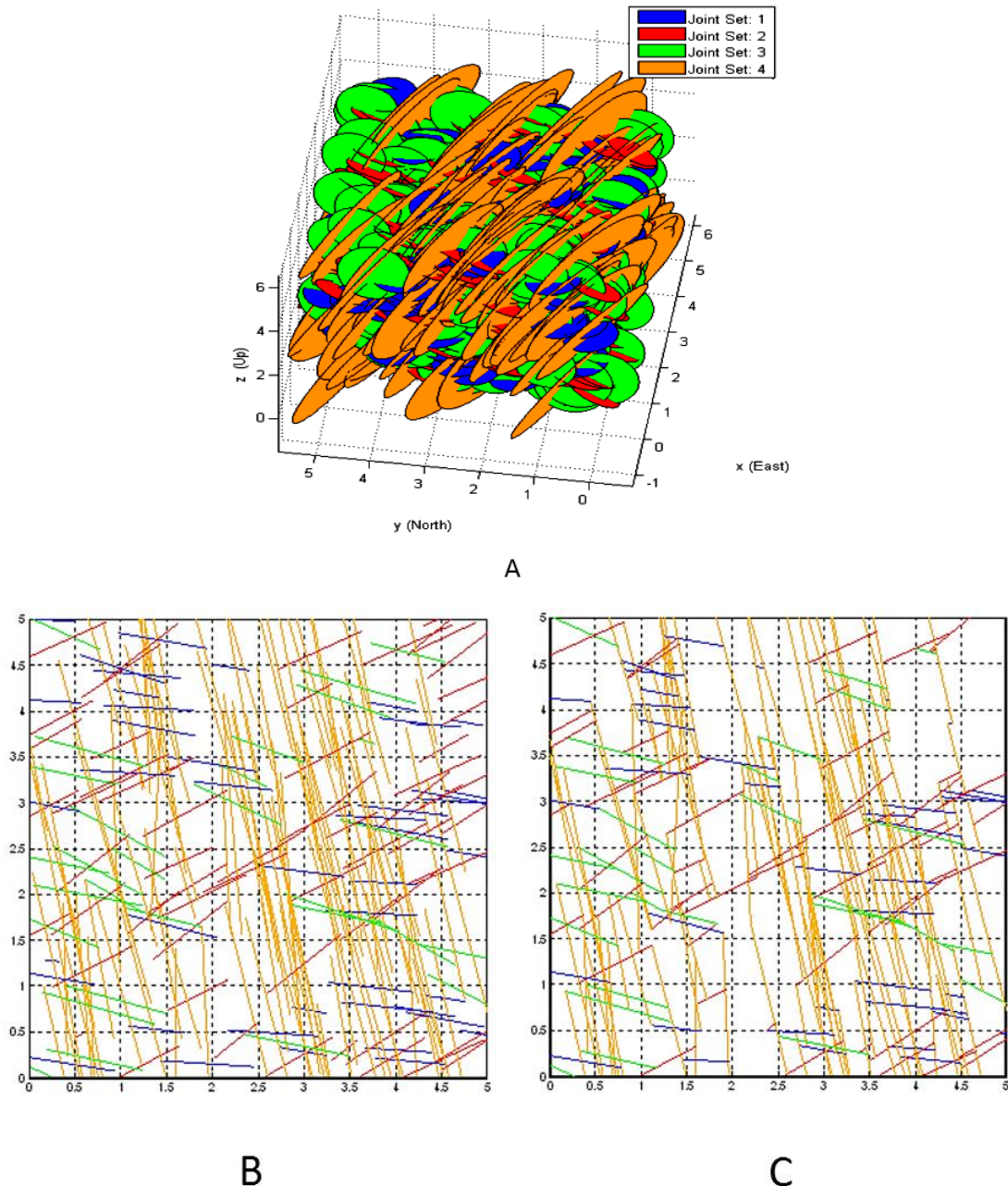


Fig. 3. ANN Data generation: A. Generated DFN by circular fractures, B. 2-D cross-section of DFN (simulated fracture traces) in non-regulated form, C. 2-D cross-section of DFN (simulated fracture traces) in a regulated form.

In order to flow analyzing in DFN, literatures mostly recommended two type of boundary condition which is prescribed on the model. In the first type of boundary condition, hydraulic gradient is assumed horizontal and flow is calculated based on the outflow of boundary 3. In the second type of boundary condition, hydraulic gradient is assumed vertical and flow is calculated

based on the outflow of boundary 4. Input and output Pressure head in both condition respectively is 5 and 1 meter. Figure 4 shows above conditions.

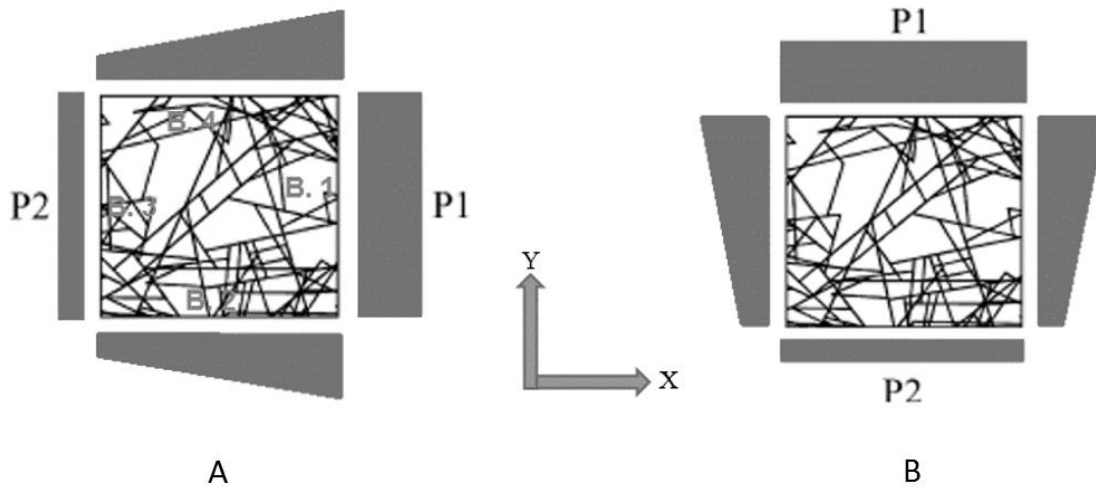


Fig. 4. Boundary conditions which are applied to DFN flow calculations: A. horizontal hydraulic gradient, B. vertical hydraulic gradient [44].

4. Optimum ANN design

In optimal neural network designing, the correct selection of input variables has a large impact on the efficiency of the network [36]. In this study, six parameters (Fisher coefficient, the length of the fractures, the standard deviation of the length of the fractures, the diameter of the fracture, the number of discontinuities in the unit length of the scan line and the opening of the fractures) were assumed as the inputs of the neural model. Given the number of input parameters, the input layer has six neurons. On the other hand, the outputs of the neural model have six parameters, namely: density of fracture intersections (P_{20}), the intensity of fracture intersection (P_{21}), frequency of permeation (ζ), conduction parameter (CP), the average exiting flow rate on the boundaries normal to the gradient direction and parallel to the horizontal flow (Q_{13}) and parallel to the vertical flow (Q_{24}), that are hydraulic parameters of the discrete fracture network. Given the number of network outputs, the output has 6 neurons. The neural network that was employed in this study is a multilayer feedforward network with backpropagation. Using the neural network toolbox of MATLAB, 50 various models of neural networks with different structures were investigated. Ultimately, the neural network model in Fig. 5 yielded the best responses with the least error and the highest correlation between model outputs and target values. Parameters and characteristics of the optimal neural network is presented in Table 2.

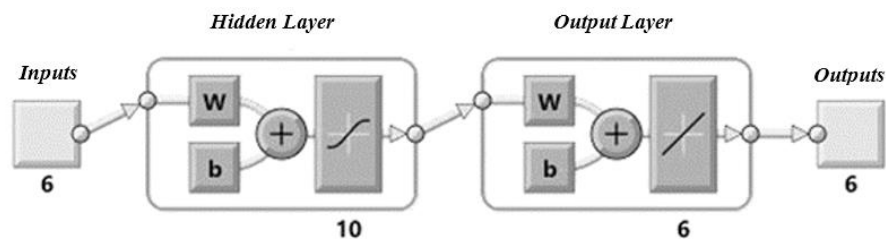


Fig. 5. Optimal designed ANN blocks.

Gradient Moments decreasing can train any network as long as its weight, net input, and transfer functions have derivative functions. Backpropagation is used to calculate derivatives of performance $perf$ concerning the weight and bias variables X . Each variable is adjusted according to gradient descent with momentum:

$$dX = mc * dX_{prev} + lr * (1 - mc) * dperf/dX \quad (5)$$

where dX_{prev} is the previous change to the weight or bias, parameter lr indicates the learning rate, derivatives of performance $dperf$ with respect to the weight and bias variables X and parameter mc is the momentum constant that defines the amount of momentum. mc is set between 0 (no momentum) and values close to 1 (lots of momentum). A momentum constant of 1 results in a network that is completely insensitive to the local gradient and, therefore, does not learn properly.

Training stops when any of these conditions occurs:

- The maximum number of epochs (repetitions) is reached.
- The maximum amount of time is exceeded.
- Performance is minimized to the goal.

Table 2

Characteristics of optimal designed ANN.

Levenberg – Marquardt	Learning Function
Gradient Moments decreasing	Weighs and bias training Algorithm
78	Total data number
2	Network layer Number
6	Input Layer Neurons Number
10	Hidden Layer Neurons Number
6	Output Layer Neurons Number

5. Results and discussion

Various methods can be used to evaluate the performance of the neural network. Mean squared error diagrams, error histograms, and also correlation coefficient between the outputs of the neural network and actual values were used in this study for evaluation of the designed neural network performance. The neural network performance was evaluated through investigation of mean squared errors by common techniques. Fig 6 shows the mean squared errors calculated for every frequency of the alternative neural network computation along with its descending development for the optimal designed neural network.

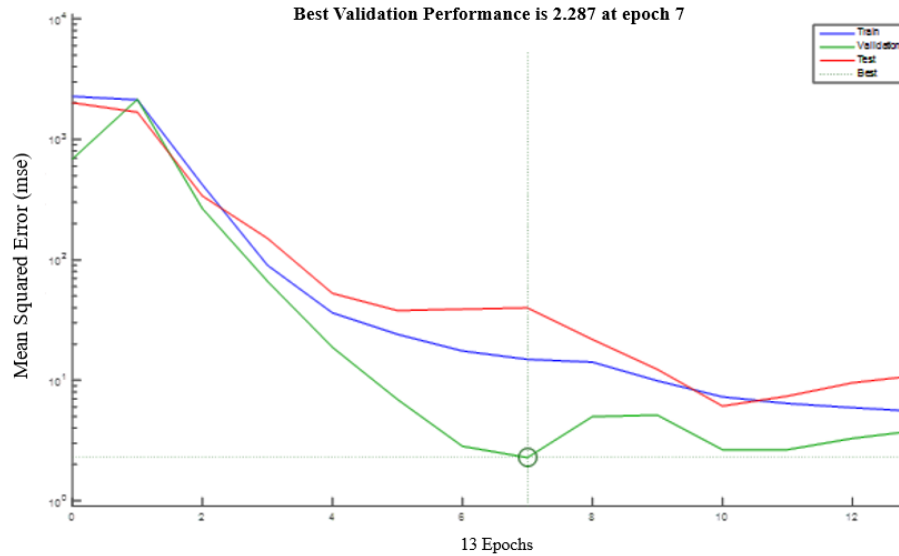


Fig. 6. Optimal designed ANN calculation epochs Mean Squared Error(MSE).

Experimental and evaluation data curves showed similar behavior proving the stability of the designed network and its reliability. According to Fig 6, the best (the least) mean squared error of evaluation data, being 2.278, was obtained at the 7th stage of the learning process. If the test data curve showed a significant increase ahead of the evaluation data, it would have implied a fault in network performance which is not seen in Fig 6.

Fig 7, shows the difference histogram for actual and computed values. Blue bars in the figure show learning data error, green bars show evaluation data error and the red bars show the network test data error. The error histogram shows the majority of error values to be between -3 and 2. Fig 7 shows that more than 90% of the data have very low errors in the range of -1.16 to 0.85. Only a few data are associated with a larger error, showing the accuracy of performance.

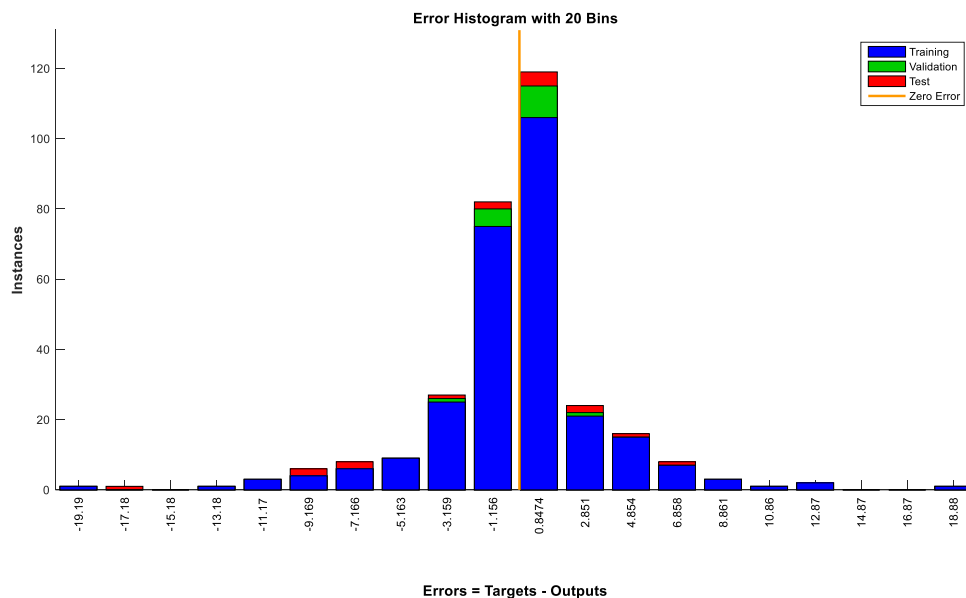


Fig. 7. Optimal designed ANN Error Histogram.

The most important metric for evaluating the performance of the neural network is the correlation between actual target data and data computed by the neural network. Fig 8 shows the correlation between actual target data and computed data for all three groups of learning, evaluation and test data.

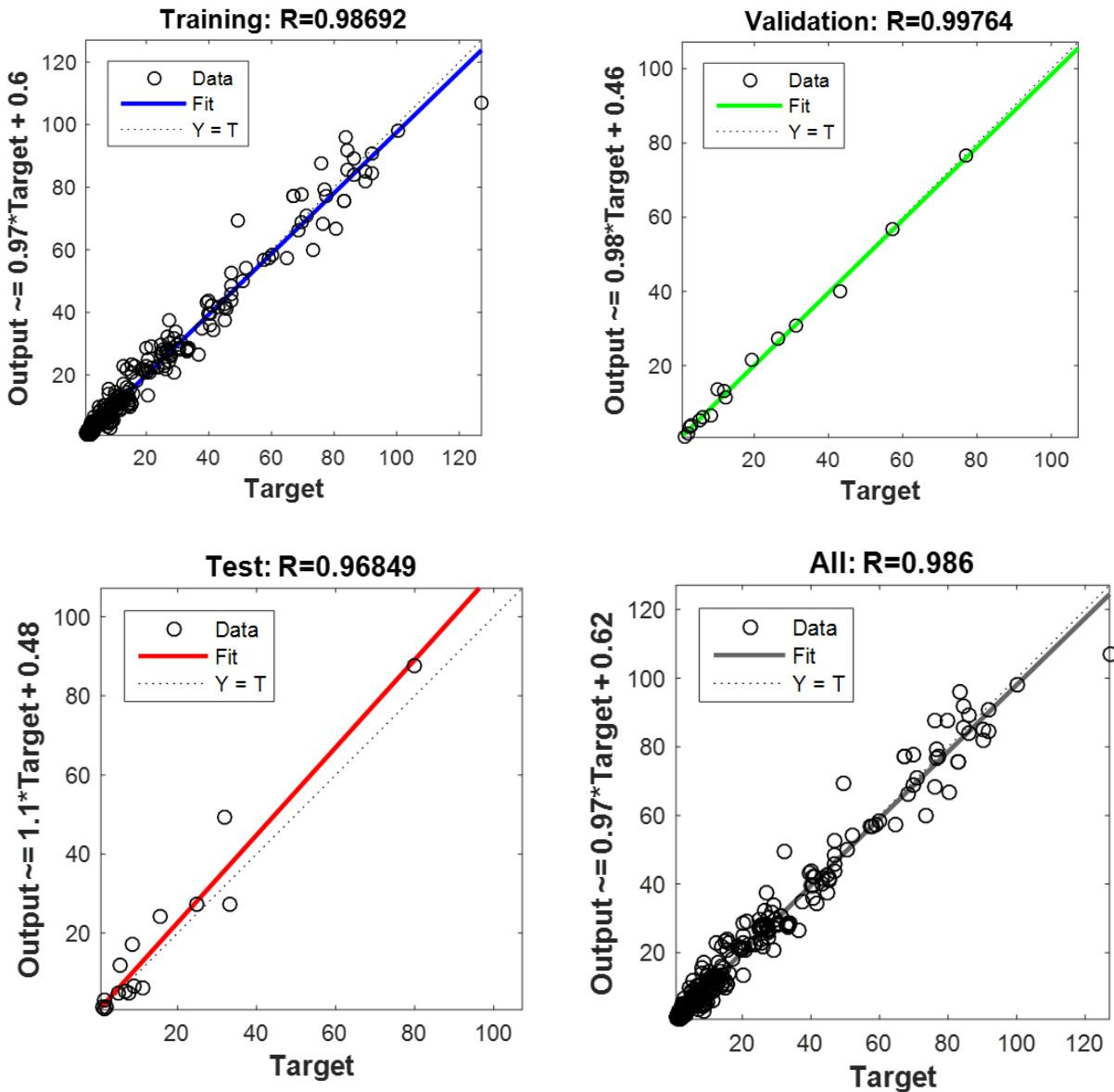


Fig. 8. Optimal designed ANN Error Histogram. Correlation Coefficient between predicted and actual data.

Diagrams in Fig 8 show an excellent correlation coefficient between actual target data and computed data. This shows the desirable performance of the designed neural network. Correlation coefficient values are very close to 1 and are presented in Table 3.

Table 3

The relation between actual and predicted value using optimal designed ANN.

The relation between predicted and actual data	Correlation Coefficient	Data type
$Pridicted\ value = 0.99 * Target + 0.6$	0.99	Training data set
$Pridicted\ value = 0.99 * Target + 0.46$	0.99	Validation data set
$Pridicted\ value = 0.97 * Target + 0.48$	0.97	Test data set
$Pridicted\ value = 0.99 * Target + 0.62$	0.99	All data

6. Conclusion

In this paper, Given the importance of hydraulic parameters of the discrete fracture network, and their time-consuming computation for dense real models, a predicting model was designed and developed drawing on the capabilities of the artificial neural network. The model predicts six hydraulic parameters upon receiving six input parameters, namely: The Fisher coefficient, length of the fractures, the standard deviation of the length of the fractures, the diameter of the fracture, the number of discontinuities in a unit length of the scan line and opening of the fractures. The hydraulic parameters are: the density of fracture intersection (P20), the intensity of fracture intersection (P21), frequency of permeation (ζ), conduction parameter (CP), average exiting flow rate on boundaries normal to fluid gradient direction (Q13), and the average existing flow rate on boundaries parallel to the fluid gradient (Q24). The discrete fracture network model was created using the developed 3DFAM software with the help of which neural network output and input parameters were computed. The high accuracy of the designed neural network provides a more accurate analysis of the hydraulic behavior of the discrete fracture network by predicting the aforementioned hydraulic parameters. Robust fitting tools that are capable of receiving multi-dimensional inputs and generating multi-dimensional outputs is a characteristic of this network.

References

- [1] Andersson J, Dverstorp B. Conditional simulations of fluid flow in three-dimensional networks of discrete fractures. *Water Resour Res* 1987;23:1876–86. doi:10.1029/WR023i010p01876.
- [2] Cacas MC, Ledoux E, de Marsily G, Tillie B, Barbreau A, Durand E, et al. Modeling fracture flow with a stochastic discrete fracture network: calibration and validation: 1. The flow model. *Water Resour Res* 1990;26:479–89. doi:10.1029/WR026i003p00479.
- [3] Long JCS, Witherspoon PA. The relationship of the degree of interconnection to permeability in fracture networks. *J Geophys Res* 1985;90:3087. doi:10.1029/JB090iB04p03087.
- [4] Ni P, Wang S, Wang C, Zhang S. Estimation of REV Size for Fractured Rock Mass Based on Damage Coefficient. *Rock Mech Rock Eng* 2017;50:555–70. doi:10.1007/s00603-016-1122-x.
- [5] Li Y, Chen J, Shang Y. Connectivity of Three-Dimensional Fracture Networks: A Case Study from a Dam Site in Southwest China. *Rock Mech Rock Eng* 2017;50:241–9. doi:10.1007/s00603-016-1062-5.
- [6] Lee C-H, Yu J-L, Hwung H-H. Fluid flow and connectivity in fractured rock. *Water Resour Manag* 1993;7:169–84. doi:10.1007/BF00872480.

- [7] Xu C, Dowd P. A new computer code for discrete fracture network modelling. *Comput Geosci* 2010;36:292–301. doi:10.1016/j.cageo.2009.05.012.
- [8] Reeves DM, Parashar R, Pohll G, Carroll R, Badger T, Willoughby K. The use of discrete fracture network simulations in the design of horizontal hillslope drainage networks in fractured rock. *Eng Geol* 2013;163:132–43. doi:10.1016/j.enggeo.2013.05.013.
- [9] Zhang Q-H, Yin J-M. Solution of two key issues in arbitrary three-dimensional discrete fracture network flow models. *J Hydrol* 2014;514:281–96. doi:10.1016/j.jhydrol.2014.04.027.
- [10] Karvounis D, Jenny P. Modeling of flow and transport in enhanced geothermal systems. Proc. 36th Work. Geotherm. Reserv. Eng. Stanford Univ. Stanford, California, 2011, p. 8.
- [11] Kvartsberg S. Hydrogeological characterisation of a fracture network, MSc Thesis, Chalmers University of Technology, Sweden. MSc Thesis, Chalmers University of Technology, Sweden, p 95, 2010.
- [12] Singhal BBS, Gupta RP. *Applied Hydrogeology of Fractured Rocks*. Dordrecht: Springer Netherlands; 2010. doi:10.1007/978-90-481-8799-7.
- [13] Fadakar-A Y, Xu C, Dowd PA. Connectivity index and connectivity field towards fluid flow in fracture-based geothermal reservoirs. Proc. 38 Work. Geotherm. Reserv. Eng. Stanford Univ. Stanford, Calif., 2013, p. 417–27.
- [14] Seifollahi S, Dowd PA, Xu C, Fadakar AY. A Spatial Clustering Approach for Stochastic Fracture Network Modelling. *Rock Mech Rock Eng* 2014;47:1225–35. doi:10.1007/s00603-013-0456-x.
- [15] Robinson PC. Connectivity of fracture systems—a percolation theory approach. *J Phys A Math Gen* 1983;16:605–14.
- [16] Englman R, Gur Y, Jaeger Z. Fluid Flow Through a Crack Network in Rocks. *J Appl Mech* 1983;50:707. doi:10.1115/1.3167133.
- [17] Charlaix E, Guyon E, Rivier N. A criterion for percolation threshold in a random array of plates. *Solid State Commun* 1984;50:999–1002. doi:10.1016/0038-1098(84)90274-6.
- [18] Stauffer D. *Introduction to Percolation Theory*. 1985.
- [19] Bour O, Davy P. Connectivity of random fault networks following a power law fault length distribution. *Water Resour Res* 1997;33:1567–83. doi:10.1029/96WR00433.
- [20] Bour O, Davy P. On the connectivity of three-dimensional fault networks. *Water Resour Res* 1998;34:2611–22. doi:10.1029/98WR01861.
- [21] Darcel C, Bour O, Davy P, de Dreuzy JR. Connectivity properties of two-dimensional fracture networks with stochastic fractal correlation. *Water Resour Res* 2003;39. doi:10.1029/2002WR001628.
- [22] Xu C, Dowd PA, Mardia K V., Fowell RJ. A Connectivity Index for Discrete Fracture Networks. *Math Geol* 2007;38:611–34. doi:10.1007/s11004-006-9029-9.
- [23] Xu C, Dowd PA, Mohais R. Connectivity analysis of the Habanero enhanced geothermal system. Proceeding, 37-th Work. Geotherm. Reserv. Eng. Stanford Univ. Stanford, Calif., 2012.
- [24] Alghalandis YF, Dowd PA, Xu C. Connectivity Field: a Measure for Characterising Fracture Networks. *Math Geosci* 2015;47:63–83. doi:10.1007/s11004-014-9520-7.
- [25] He J, Chen S, Shahrour I. Back Analysis of Equivalent Permeability Tensor for Fractured Rock Masses from Packer Tests. *Rock Mech Rock Eng* 2011;44:491–6. doi:10.1007/s00603-011-0149-2.
- [26] Benardos AG, Kaliampakos DC. Modelling TBM performance with artificial neural networks. *Tunn Undergr Sp Technol* 2004;19:597–605. doi:10.1016/j.tust.2004.02.128.

- [27] Bowden GJ, Dandy GC, Maier HR. Input determination for neural network models in water resources applications. Part 1—background and methodology. *J Hydrol* 2005;301:75–92. doi:10.1016/j.jhydrol.2004.06.021.
- [28] Kingston GB, Maier HR, Lambert MF. Bayesian model selection applied to artificial neural networks used for water resources modeling. *Water Resour Res* 2008;44. doi:10.1029/2007WR006155.
- [29] Kung TC, Hsiao CL, Schuster M, Juang CH. A neural network approach to estimating excavation-induced wall deflection in soft clays. *Comput Geotech* 2007;34:385–96.
- [30] Kim CY, Bae GJ, Hong SW, Park CH, Moon HK, Shin HS. Neural network based prediction of ground surface settlements due to tunnelling. *Comput Geotech* 2001;28:517–47. doi:10.1016/S0266-352X(01)00011-8.
- [31] Padmini D, Ilamparuthi K, Sudheer KP. Ultimate bearing capacity prediction of shallow foundations on cohesionless soils using neurofuzzy models. *Comput Geotech* 2008;35:33–46. doi:10.1016/j.compgeo.2007.03.001.
- [32] Kulatilake PHSW, Qiong W, Hudaverdi T, Kuzu C. Mean particle size prediction in rock blast fragmentation using neural networks. *Eng Geol* 2010;114:298–311. doi:10.1016/j.enggeo.2010.05.008.
- [33] Monjezi M, Amiri H, Farrokhi A, Goshtasbi K. Prediction of Rock Fragmentation Due to Blasting in Sarcheshmeh Copper Mine Using Artificial Neural Networks. *Geotech Geol Eng* 2010;28:423–30. doi:10.1007/s10706-010-9302-z.
- [34] Nejati HR, Ghazvinian A, Moosavi SA, Sarfarazi V. On the use of the RMR system for estimation of rock mass deformation modulus. *Bull Eng Geol Environ* 2014;73:531–40. doi:10.1007/s10064-013-0522-3.
- [35] Gokceoglu C, Sonmez H, Kayabasi A. Predicting the deformation moduli of rock masses. *Int J Rock Mech Min Sci* 2003;40:701–10. doi:10.1016/S1365-1609(03)00062-5.
- [36] Fausett L V. *Fundamentals of neural networks: architectures, algorithms, and applications*, Prentice-Hall, Englewood Cliffs, New Jersey. Prentice-hall Englewood Cliffs; 1994.
- [37] Demuth H, Beale M, Hagan M. *Neural Network Toolbox for use with MATLAB. User's Guid Version 5 MathWorks, Inc* 2015.
- [38] Shahin MA. State-of-the-art review of some artificial intelligence applications in pile foundations. *Geosci Front* 2016;7:33–44. doi:10.1016/j.gsf.2014.10.002.
- [39] Zurada JM. *Introduction to artificial neural systems*. West Publishing Company, St. Paul; 1992.
- [40] Zheng J, Deng J, Zhang G, Yang X. Validation of Monte Carlo simulation for discontinuity locations in space. *Comput Geotech* 2015;67:103–9. doi:10.1016/j.compgeo.2015.02.016.
- [41] Rouleau A, Gale JE. Statistical characterization of the fracture system in the Stripa granite, Sweden. *Int J Rock Mech Min Sci Geomech Abstr* 1985;22:353–67. doi:10.1016/0148-9062(85)90001-4.
- [42] Leung CTO, Zimmerman RW. Estimating the Hydraulic Conductivity of Two-Dimensional Fracture Networks Using Network Geometric Properties. *Transp Porous Media* 2012;93:777–97. doi:10.1007/s11242-012-9982-3.
- [43] Kemeny J, Post R. Estimating three-dimensional rock discontinuity orientation from digital images of fracture traces. *Comput Geosci* 2003;29:65–77. doi:10.1016/S0098-3004(02)00106-1.
- [44] Baghbanan A. *Scale and stress effects on hydro-mechanical properties of fractured rock masses*, Ph. D. Dissertation, KTH land and water Resources Engineering, Swede. KTH, 2008.